Univerza v *Ljubljani*
Fakulteta za *matematiko in fiziko*

Oddelek za fiziko

Seminar I_b - 1. letnik, II. stopnja

Animal locomotion on the water surface

Author:
Mitja Zidar

Advisor:
prof. dr. Rudolf Podgornik

Ljubljana, May 7, 2015

Abstract

This seminar describes physical phenomena related to surface tension, such as menisci and capillary waves, that influence animals living atop the water surface, and the means by which they are exploited by these animals for locomotion.

Contents

1 Introduction **2**

2 Surface tension **2**

3 Propulsion **4**
3.1 Capillary waves 4
3.2 Water strider propulsion 6

4 Climbing the meniscus **7**

5 Conclusion **11**

1 Introduction

Many animals have mastered the enviable act of walking on water through the use of surface tension. Many of those have evolved to live on the water surface almost exclusively, living, hunting, even reproducing on the calm surfaces of ponds, rivers, lakes and the sea. Such are the animals of the family *Gerridae*, which are more commonly known as water striders [1]. These are animals which range in size from a couple of millimetres to well over 20 centimetres whose physiology is uniquely suited to life on such vast slippery plains.

Figure 1: Water strider *Gerris remigis*. Scale bar, 1 cm. Adopted from [1]

2 Surface tension

Surface tension arises from the fact that the sum of the forces on the water (or any other liquid) molecule at the surface differs from the total force on the molecule in the bulk, leading to a finite surface energy in the form

$$W_\mathrm{s} = \sigma S, \tag{2.1}$$

where S is the liquid surface and σ is surface tension $\left[\frac{\mathrm{N}}{\mathrm{m}}\right]$. Because of strong interaction between water molecules provided by the hydrogen bond network between them, water has a high surface tension (72.8 mN/m at 20 °C) compared to that of most other liquids (for toluene, ethanol, acetone $\sigma \approx 20$ mN/m [2]).

Consider a surface (unit outward normal $\hat{n}$) of a liquid of density ρ in the vicinity of a long, straight obstacle (e.g. wall, or a water-strider's leg) at position $x = 0$. Let $\eta(x) = z$ be the deviation from a flat surface caused by the obstacle. The balance between hydrostatic and curvature pressures are expressed by the Young-Laplace equation (2.2)

$$\rho g \eta = \sigma \nabla \cdot \hat{n}. \tag{2.2}$$

The boundary condition for this equation is the angle θ of the water surface relative to the horizontal (as defined in Fig. 2) at the water—obstacle contact at $x = 0$. This angle is determined by obstacle orientation (the angle of the obstacle surface facing the water) and the contact angle, which is in turn determined by the nature of interaction between molecules of water and the obstacle (hydrophobic or hydrophilic). Angle θ is positive if the surface is curved upward and negative if it is curved downward.

By further assuming that the incline is everywhere sufficiently small $\left(\frac{\partial \eta}{\partial x} \ll 1\right)$, Eq. (2.2) yields a meniscus shape of

$$\eta(x) = l_\mathrm{c} \tan\theta \mathrm{e}^{-x/l_\mathrm{c}}, \tag{2.3}$$

where l_c is the capillary length

$$l_\mathrm{c} = \sqrt{\frac{\sigma}{\rho g}} \tag{2.4}$$

and equals around 30 mm in water. The vertical component of force per unit length on such an obstacle is

$$F_\mathrm{z} = \sigma \sin\theta.$$

Water striders' legs are covered by thousands of hairs, making them effectively non-wetting. This way they can deform the water surface in such a way that it supports their weight through surface tension as is shown in Fig. 2.

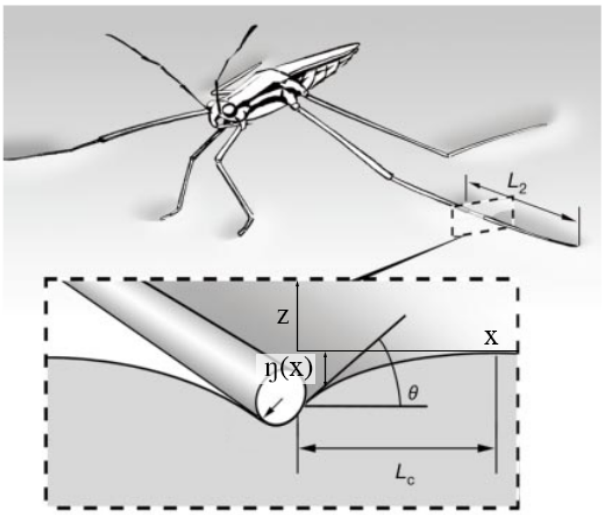

Figure 2: a water strider on the surface. The force per unit length applied on any of its hydrophobic limbs cannot exceed 2σ, lest its legs pass through the surface. As the striders increase in size, their legs therefore become proportionately longer. Adopted from [1].

3 Propulsion

3.1 Capillary waves

The driving force behind large waves on the water surface is gravity. Gravity is the restoring force that tends to flatten out the bulges in a curving surface. But on scales of one centimetre or less, gravity is not the dominant force any more. Capillary waves, or ripples, that affect surface aquatic animals, are mainly driven by surface tension. In this section we will calculate the phase speed and momentum of capillary waves (in the derivation I have relied heavily on [3]).

Consider a body of water on the surface of the Earth ($g = 9.81$ m/s^2). Suppose that x measures horizontal distance and z measures vertical height, with $z = 0$ corresponding to the flat surface of water. We assume that there is no motion in the y direction.

Because of effective incompressibility of water at phase speeds of surface waves, the continuity equation everywhere in the liquid (surface and bulk) is reduced to

$$\frac{\partial v_{\mathrm{x}}}{\partial x} + \frac{\partial v_{\mathrm{z}}}{\partial z} = 0. \tag{3.1}$$

Let $p(x, z, t)$ be the pressure in the water. Newton's second law states

$$\rho \frac{\partial v_{\mathrm{x}}}{\partial t} = -\frac{\partial p}{\partial x}, \tag{3.2}$$

$$\rho \frac{\partial v_{\mathrm{z}}}{\partial t} = -\frac{\partial p}{\partial z} - \rho g, \tag{3.3}$$

the difference between x and z directions being that water is subject to a downward acceleration due to gravity. We can write

$$p = p_0 - \rho g z + p_1,$$

where p_0 is the atmospheric pressure and p_1 is the pressure perturbation due to the wave. Substitution into equations (3.2) and 3.3 and derivation of these equations with respect to z and x, respectitavely, yields

$$\rho \frac{\partial}{\partial t}\left(\frac{\partial v_{\mathrm{x}}}{\partial z} - \frac{\partial v_{\mathrm{x}}}{\partial z}\right) = 0$$

or

$$\frac{\partial v_{\mathrm{x}}}{\partial z} - \frac{\partial v_{\mathrm{x}}}{\partial z} = 0. \tag{3.4}$$

(Actually, this quantity could be non-zero and constant in time, but this is not consistent with an oscillating wave-like solution.) Eq. (3.4) indicates that we can at this point introduce a velocity potential ϕ:

$$v_{\mathrm{x}} = \frac{\partial \phi}{\partial x},\ v_{\mathrm{z}} = \frac{\partial \phi}{\partial z}.$$

Finally, equations (3.2) and (3.3) yield

$$p_1 = -\rho \frac{\partial \phi}{\partial t}. \tag{3.5}$$

Potential ϕ can be obtained from Eq. 3.1, which is now Laplace's equation,

$$\triangle\phi = 0 \tag{3.6}$$

We can now introduce surface tension. Because of it, there is a small pressure discontinuity across a curved surface:

$$p_{\mathrm{st}} = \sigma\frac{\partial^2\eta}{\partial x^2},$$

where the second derivative represents a reciprocal value of the radius of curvature of the surface. The Laplace's equation (3.6) must thus satisfy a boundary condition

$$\sigma\frac{\partial^2\eta}{\partial x^2} = \rho g\eta - p_1|_{z=0}.$$

We are looking for a propagating wave-like solution in the form of

$$\phi(x,z,t) = A\mathrm{e}^{kz}\cos(\omega t - kx). \tag{3.7}$$

Note that the second boundary condition, the "deep water" condition is already satisfied by the solution in the form of Eq. (3.7) because of its exponential decay with increasing depth ($z < 0$). By inserting Eq (3.7) into the Laplace equation we finally get the phase velocity of surface waves

$$v_{\mathrm{ph}}^2 = \frac{\sigma k}{\rho} + gk. \tag{3.8}$$

The first part describes the effect of surface tension and the second part describes the effect of gravity. On a scale of about a centimetre the contributions are roughly equal while on a millimetre scale the influence of gravity is already smaller by an order of magnitude (i.e. proper capillary waves).

Having calculated the dispersion relation of capillary waves, let us now consider their momentum. The momentum of a wave packet is given by

$$\vec{P} = \frac{E}{v_{\mathrm{ph}}}\hat{k},$$

where $E = W_{\mathrm{s}}$ is the total energy the wave packet is carrying. The energy of a capillary wave is stored in the enlarged liquid surface due to its sinusoidal (instead of flat) form. For a single wavelength of a plane wave of a lateral extent W the Eq. (2.1) is written as

$$E = W\Delta l\sigma,$$

where Δl is the difference in (surface) length of the sinusoidal wave compared to the flat surface. For infinitesimal amplitude it is calculated as

$$\Delta l = \int_0^\lambda \sqrt{1 + \left(\frac{\mathrm{d}\eta}{\mathrm{d}x}\right)^2} - 1\ \mathrm{d}x \approx \frac{1}{2}\int_0^\lambda \left(\frac{\mathrm{d}\eta}{\mathrm{d}x}\right)^2 \mathrm{d}x.$$

Using the sinusoidal waveform as η, amplitude a and the dispersion relation (3.8), the expression for momentum carried by a single wave of lateral length W is

$$P = a^2\pi W\sqrt{k\sigma\rho}, \tag{3.9}$$

where k is the magnitude of the wave vector $\frac{2\pi}{\lambda}$.

3.2 Water strider propulsion

In order for the water strider to move, it has to somehow transfer the momentum of its legs to the underlying liquid. It has long been thought that generation of momentum via capillary waves was the sole mean of such propulsion. To produce such waves, the water strider needs only to skim the surface with a back and forth motion, pushing away a negligible amount of water in the process. But with the help of previously derived equations we can show that this cannot be the case.

A water strider of mass $m \approx 0.01$ g achieves a characteristic speed of v =100 cm/s, meaning that it generates a momentum of $P = mv \approx 1$g cm/s with a single stroke. The measurements, on the other hand, have indicated that each leg stroke produces a capillary wave packet of about three waves with wavelength λ and amplitude a a couple of millimetres. Their width was measured to be around $W \approx 0.3$ cm [1]. Using Eq. (3.9) we can calculate the momentum of such a wave package to be roughly $P \approx 0.1$ g cm/s — an order of magnitude less that the momentum of the strider.

The solution has come from careful observations of high speed videos of a moving water strider, which have shown a series of small hemispherical dipolar vortices in its wake (as shown in Fig. 4 and Fig. 3) not dissimilar to vortices in the wake of a rowing boat and moving backwards at a characteristic speed of $v_\mathrm{v} \approx 4$ cm/s. The radii of the vortices were measured to be $r_\mathrm{v} \approx 0.4$ cm (mass $m_\mathrm{v} = 2\rho\pi r_\mathrm{v}^3/3$), giving a pair of such vortices a total momentum of $P = 2m_\mathrm{v}v_\mathrm{v} \approx 1$ g cm/s. The vertical extent of r_v is much greater than the static meniscus depth of the driving legs (120 μm), but comparable to the maximum depth of the meniscus at which the leg would penetrate the surface (0.1 cm). This suggests that the water strider uses its legs as paddles and the adjoining menisci as blades — pushing the legs as deep as possible without sinking and using the leg's menisci to propel water backwards.

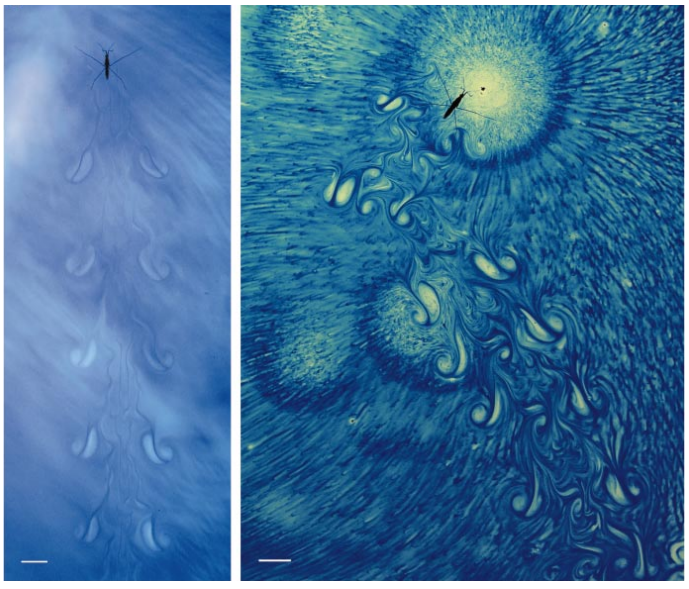

Figure 3: vortices, captured with the help of a thin layer of thymol blue on the surface of the water. Scale bars, 1 cm. Adopted from [1].

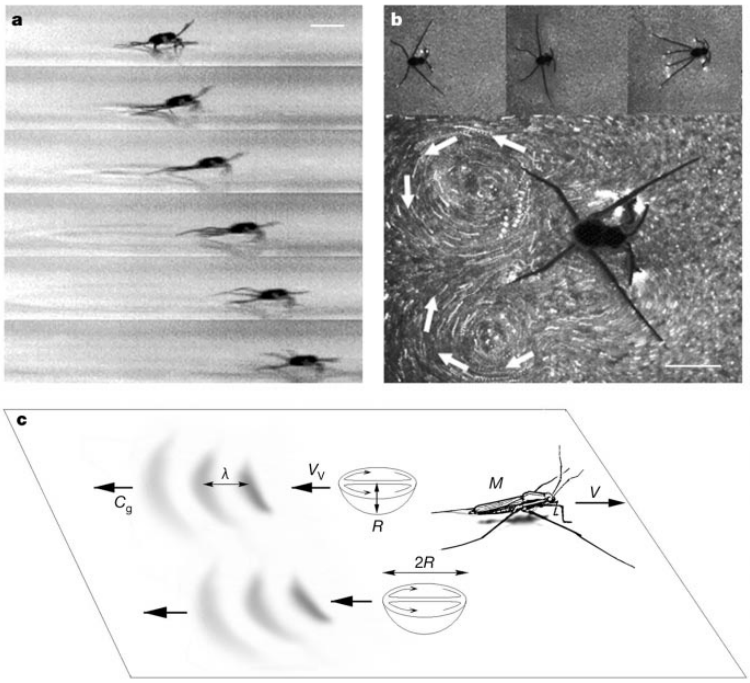

Figure 4: the rowing motion of a water strider and the vortices it creates. The capillary waves are mostly just a bi-product, carrying away a negligible part of the transferred momentum. Scale bars, 1mm. Adopted from [1].

4 Climbing the meniscus

Surface-dwelling animals must cross the border between land and water on a regular basis; to lay eggs or to escape from predators, for example. But to achieve this they must somehow climb the frictionless slope of meniscus at the water's edge. The task is simple for animals which are much larger than the characteristic length of l_c (Eq. (2.4)). But many millimetre scale animals are unable to simply stride over the slippery slope. Through evolution, they have thus developed an ingenious technique of climbing the meniscus by assuming a fixed body posture without even moving their appendages.

Figure 5: The attractive force holding two floating paper-clips together and the grouping of bubbles at the glass' edge are both caused by surface tension.

The lateral forces acting between objects floating on the surface have long been known to physicists (Fig. 5). These forces are caused by interaction between particles through deformation of the surface. The interfacial profile around two floating particles can be written as a linear combination of profile functions appropriate to the isolated particles. Provided the interfacial slope is everywhere sufficiently small and that particles themselves are small (point force) the profile is simply the sum of both functions [5]. When two floating particles approach each other they thus influence each other through a change in gravitational potential energy, and the force of the second particle on the first particle is simply calculated as

$$\vec{F}_{21}(x) = -\frac{\partial E(x)}{\partial \vec{r}} = -F_{1z}\frac{\partial \eta_2(x)}{\partial \vec{r}}, \tag{4.1}$$

where $F_{1z}\hat{z}$ is the vertical force of the first particle (e.g. weight) and $\eta_2(x)$ is the interfacial profile of an isolated second particle. The problem is equivalent to an object on a frictionless slope (see Fig. 6).

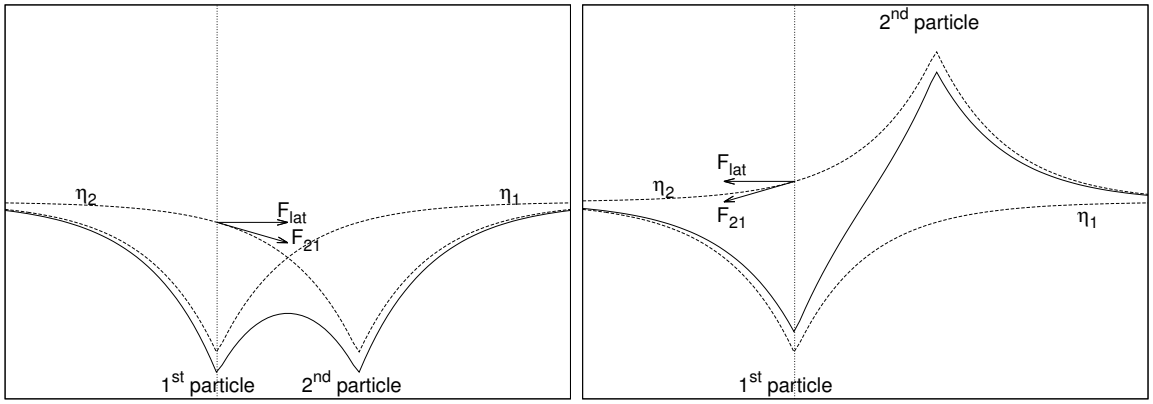

Figure 6: interfacial profile around two objects that exert vertical force on the water surface in the same direction (left) and in opposite directions (right). The lateral force between the objects in the first case (e.g. two paper-clips) will be attractive. In the second case (e.g. a paper-clip and a bubble), the lateral force is repulsive. If the the interfacial slope is everywhere sufficiently small the magnitude of lateral force F_{lat} is almost equivalent to F_{12} [5].

Let a hydrophillic wall (e.g. a floating log) on the edge of the water now take on the roll of the second particle and the first particle be a small, massless object at distance x_0 from the edge and acting on the surface with the vertical force $F_z\hat{z}$. By combining Eq. 2.3 which describes the meniscus shape near such a wall and Eq. 4.1 we get

$$\vec{F}(x_0) = -F_z \tan\theta e^{-x_0/l_c}\hat{x}. \tag{4.2}$$

An object pushing into the surface ($F_z < 0$) of a meniscus will thus slide down the slope; however by pulling the surface upward ($F_z > 0$) it will be drawn up the slope. An insect can exploit this fact by using its front and rear tarsi, equipped with hydrophilic claws, to pull the water surface up (force F_1 with the front tarsi and F_3 with the back) and its hydrophobic middle tarsi to push down (F_2), as dictated by the force balance. By applying the majority of upward force to the front legs and stretching out the back legs as far as

possible (to balance the torque) the insect takes advantage of the exponentially curved surface to achieve negative net force that draws it up the slope, as is shown in Fig. 7.

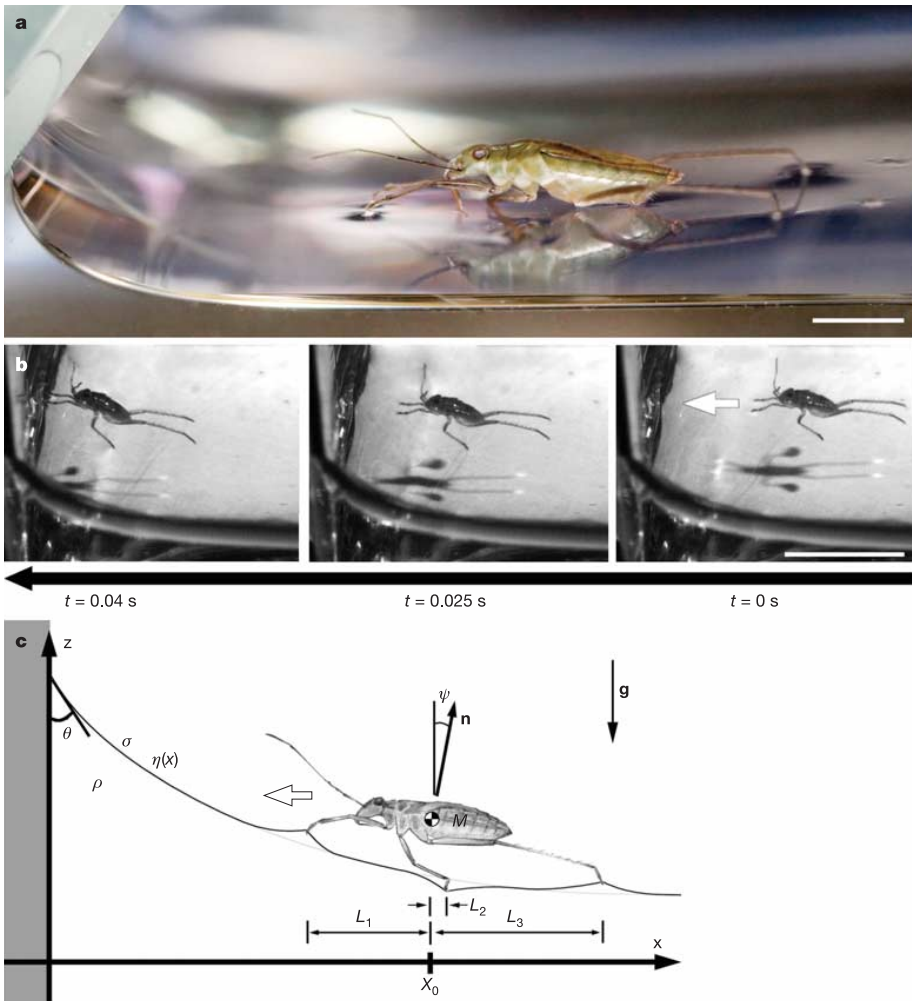

Figure 7: Meniscus climbing by the water treader *Mesovelia* (weight 2 μN). Note the pulling with the front and hind legs and pushing with the middle legs. In pulling up the insect forms a meniscus that generates a bright spot on the floor, and in pushing it down it casts a shadow. Characteristic speed of ascent is a couple of cm/s and the corresponding F_1 (see Eq. (4.3)) was calculated to be about 20-40 μN. Scale bars, 3mm. The bottom picture illustrates the physical model of the ascent. Adopted from [6].

Consider an insect shown in this figure, of mass M with the center of mass at point x_0 from the edge of the water. We assume that the meniscus slope is small ($\sin\psi \approx \tan\psi \approx -\dot{\eta}(x)$) and does not change considerably over the length of the insect. The force balance in the z axis is

$$F_2 = F_1 + F_3 + Mg.$$

The torque balance about the insect's middle legs is

$$F_3 L_3 = F_1 L_1 - MgL_2.$$

Using Eq. 4.2, the driving force in tangential direction produced by the legs can be expressed as

$$F(x_0) = -\tan\theta \mathrm{e}^{-x_0/lc}\left(F_1\mathrm{e}^{L_1/lc} + F_3\mathrm{e}^{-L_3/lc} - F_2\mathrm{e}^{-L_2/lc}\right).$$

This force is balanced out by the tangential component of gravitational force and acceleration. The tangential force balance on the insect is

$$M\frac{\mathrm{d}^2x_0}{\mathrm{d}t^2} = -\tan\theta \mathrm{e}^{-x_0/lc}\left(F_1\mathrm{e}^{L_1/lc} + F_3\mathrm{e}^{-L_3/lc} - F_2\mathrm{e}^{-L_2/lc} - Mg\right). \tag{4.3}$$

The acceleration is negative (i.e. the bug travels up the slope) if the effect of pulling with front and hind legs is greater than the push with middle legs and the tangential component of gravitational pull. Some terrestrial animals have mastered this ability without having legs especially suited to manipulate the water surface, as is shown in Fig. 8. They use their whole body to deform the surface, but they still use the same principle given by Eq. 4.3.

Although the validity of this equation breaks down with higher contact angles it can still be used to illustrate qualitatively the meniscus climbing ability. This ability is unique in a sense that an animal does not transfer its muscular strain energy directly into kinetic and gravitational energy of itself and the kinetic energy of surrounding fluid, but instead it stores the energy into deformation of the free surface that powers its ascent.

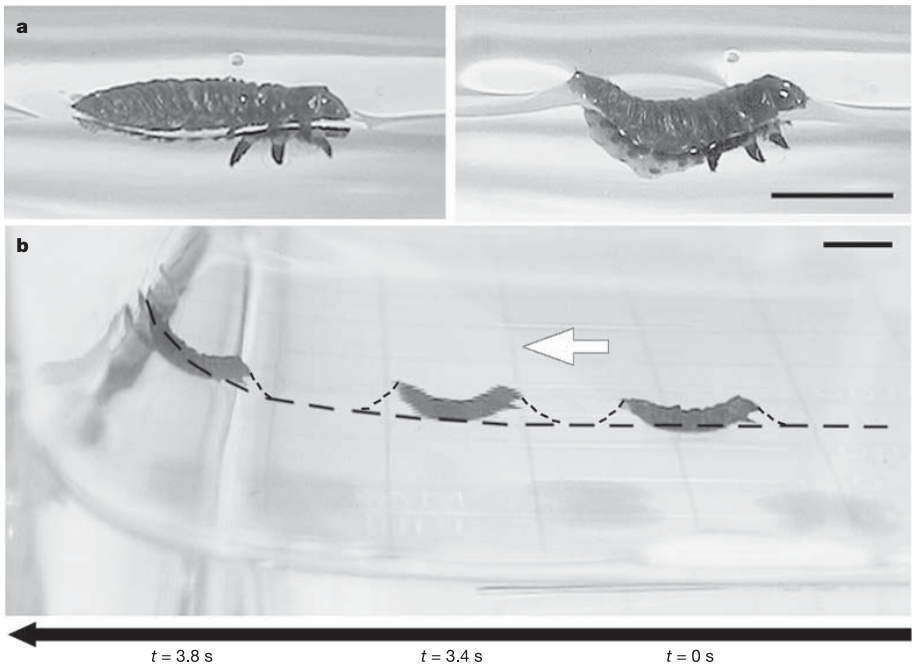

Figure 8: Meniscus climbing by the larva of the waterfly leaf beetle (weight 1.5 mN). Although a terrestrial insect, it has nevertheless developed a meniscus-climbing ability for survival purposes. It deforms the surface by arching its back. The corresponding F_1 was calculated to be about 0.2 mN. Scale bars, 3 mm. Adopted from [6].

5 Conclusion

The basics of animal locomotion on the water surface have been mostly unlocked by scientists and researchers from around the world. This is best illustrated by the construction of the mechanical Robostrider (Fig 9) by the Department of Mechanical engineering of MIT. However the style of locomotion, far less elegant than that of its natural counterpart, leaves much to be desired. The maximum speed of the spring-powered Robostrider is only about a third of the common *Gerridae*, not to mention that a single winding takes it only about 20 cm far [1].

The problem of water walking seems as intriguing and complicated as the related conundrum of insect flight. The insects too have puzzled the scientist for generations with their perfected technique of flapping which continues to evade all but the most complicated aerodynamic explanations. There too, vortices and vortex shedding seem to be play a major role in propulsion. What is more, in addition to the shed vortices which carry the brunt of the momentum keeping the insect aloft, a prominent leading edge vortex remains stably attached on the insect wing throughout the flapping cycle and does not shed into the wake, as it would from simple non-flapping wings (or rudimentary Robostrider's rigid metallic legs). Its presence, combined with other mechanisms acting during changes in angle of attack, greatly enhances the forces generated by the wing, thus thwarting most of the engineers' attempts to replicate an insect wing [7].

The evolution has equipped humble insects that populate air and water alike with a keen understanding of hydrodynamics which humans are just now beginning to get a grip of. Our machines that operate at those scales are cumbersome at best because simply adding more engine power, which we are accustomed to do with machines that serve us in everyday life, just does not cut it when it comes to delicate movement of insects' appendages. What is needed is a deeper hydrodynamic understanding of those movements and intricate mechanics to exploit it. And scientists are getting closer every day.

Figure 9: An adult water strider facing its larger mechanical counterpart. Robostrider mimics the motion of a water strider by using both waves and vortices as means of propulsion. Scale bars, 1 cm. Adopted from [1]

References

[1] D.L. Hu, J. W. M. Bush, Nature, Vol. 424, pp. 663 to 666 (2003).

[2] Lange's Handbook of Chemistry , 10th ed. (1967)

[3] http://farside.ph.utexas.edu/teaching/315/Waves (19.2.2015)

[4] K. E. Kenyon, Journal of Oceanography, Vol. 54, pp. 343 to 346 (1998).

[5] D. Y. C. Chan, J. D. Henry, L. R. White, The Interaction of Coloidal Particles Collected at Fluid Interfaces (1980)

[6] D.L. Hu, D. Chen, J. W. M. Bush, Nature, Vol. 437, pp. 733 to 736 (2005).

[7] S. P. Sane, The Journal of Experimental Biology, Vol. 206, pp. 4191-4208 (2003)